Verdet constant dispersion of magnesium fluoride for deep-ultraviolet and vacuum-ultraviolet Faraday rotators

Research Article Vol. 31, No. 5 / 27 Feb 2023 / Optics Express 7807
Optics EXPRESS

Verdet constant dispersion of magnesium fluoride for deep-ultraviolet and vacuum-ultraviolet Faraday rotators

YUKI TAMARU,[1,2,4] ATSUSHI FUCHIMUKAI,[2] HIYORI UEHARA,[1,3] TAISUKE MIURA,[2] AND RYO YASUHARA[1,3,*]

[1]SOKENDAI (The Graduate University for Advanced Studies), 322-6 Oroshi-cho, Toki, Gifu 509-5292, Japan
[2]Gigaphoton Inc., 400 Yokokurashinden, Oyama, Tochigi 323-8558, Japan
[3]National Institutes of Natural Sciences, National Institute for Fusion Science, 322-6 Oroshi-cho, Toki, Gifu 509-5292, Japan
[4]tamaru.yuki@nifs.ac.jp
[*]yasuhara.ryo@nifs.ac.jp

Abstract: The Verdet constant dispersion in magnesium fluoride (MgF_2) crystals was evaluated over a wavelength range of 190–300 nm. The Verdet constant was found to be 38.7 rad/(T·m) at a wavelength of 193 nm. These results were fitted using the diamagnetic dispersion model and the classical Becquerel formula. The fitted results can be used for the designing of suitable Faraday rotators at various wavelengths. These results indicate the possibility of using MgF_2 as Faraday rotators not only in deep-ultraviolet regions, but also in vacuum-ultraviolet regions owing to its large bandgap.

1. Introduction

The Faraday effect is a magneto-optical effect, in which the polarization plane of an electromagnetic wave is rotated proportionally to the applied magnetic field strength. Faraday rotators (FR) based on this effect are widely used in optical isolators [1,2], magnetic and electric current sensors [3,4], and tunable bandpass filters [5]. The polarization rotation angle θ_F is proportional to the magnetic field strength B and the length of the medium l and can be expressed as follows:

$$\boldsymbol{\theta_F}(\boldsymbol{\lambda}) = V(\boldsymbol{\lambda}) \int_0^l \boldsymbol{B}\boldsymbol{dl}, \tag{1}$$

where V denotes the Verdet constant, which depends on the medium and the wavelength. This value at each wavelength is an important parameter to design appropriate FR for any application. Several materials exist for FRs in visible and/or infrared wavelengths because the use of optical isolators is crucial for high-power lasers, such as Nd:YAG lasers, at a wavelength of 1064 nm to prevent laser damage and unwanted feedback to the laser oscillator through returning light. However, in a shorter-wavelength region, only a few materials have been reported as candidate FR materials. Lately, the importance of deep-ultraviolet (DUV: λ = 190–400 nm) light has increased with the development of frequency conversion by nonlinear crystals, solid-state lasers, and blue laser diodes [6–8].

In addition, several light sources have been reported in the short-wavelength regions of the vacuum-ultraviolet regions (VUV: below λ = 200 nm) [9–11]. Therefore, the Verdet constant of various candidate materials in DUV and VUV regions is an important insight into various laser light sources at different laser specification such as output power and pulse duration. Phosphates (potassium dihydrogen phosphate (KDP), deuterated potassium phosphate (DKDP), and ammonium dihydrogen phosphate (ADP)) were studied as candidate materials because they exhibit high transmittance and have high Verdet constants (V_{KDP} = 67.6 rad/(T·m), V_{DKDP} = 74.5 rad/(T·m),

#481745 https://doi.org/10.1364/OE.481745
Journal © 2023 Received 23 Nov 2022; revised 28 Dec 2022; accepted 30 Dec 2022; published 16 Feb 2023

Optics EXPRESS

V_{ADP} = 70.2 rad/(T·m) at λ = 193 nm) in DUV regions [12]; however, these materials are soft and hygroscopic. Recently, synthetic quartz (SQ) glass has been reported as a candidate material because it exhibits high transparency without a transitional absorption line and has a high Verdet constant (V_{SQ} = 70.1 rad/(T·m) at λ = 193 nm) [13,14]. Among the candidate materials, fluoride crystals are considered as the most promising materials that exhibit high transparency in DUV regions owing to their large bandgaps. CeF_3 and PrF_3 were reported as candidate materials in UV-visible regions (V_{CeF3} = 1146 rad/(T·m) at λ = 308 nm, V_{PrF3} = 2964 rad/(T·m) at λ = 222 nm) [15]. In particular, optical isolators based on CeF_3 at wavelengths of 355 nm and 405 nm were reported [16]. However, these two materials exhibit a relatively longer cutoff wavelength (λ = 210 nm for PrF_3 and λ = 306 nm for CeF_3) compared to that of other fluoride crystals, complicating their use across entire DUV regions. $LiREF_4$ (RE = Tb, Dy, Ho, Er, and Yb) has been reported to have a high Verdet constant owing to the rare-earth contribution and short cutoff wavelength [17]; although, these materials exhibit several rare-earth absorption lines in DUV regions. Yttrium lithium fluoride ($LiYF_4$, YLF) crystal has been reported as a candidate material for use in VUV regions because of its short absorption edge (V_{YLF} = 63.7 rad/(T·m) at λ = 157 nm) [18]. Among other fluoride crystals, magnesium fluoride (MgF_2) crystals have wide band gaps (10.8 eV) and high transmittance from wavelengths of 110 nm [19,20]. Although the Verdet constant has been reported in the visible region [21], no data exist for DUV and VUV regions. In this study, the wavelength dispersion of the Verdet constant in MgF_2 was evaluated in a wavelength range of 190–300 nm.

2. Experimental methods

The experimental setup for the Verdet constant dispersion measurements is shown in Fig. 1. The measurement scheme is similar to that of the polarization stepping method [22]. A white light beam (λ = 170-2100 nm), obtained from an optical discharge plasma light source (Energetiq Technology Inc. EQ-99X LDLS), was linearly polarized using the first DUV Wollaston Glan Taylor polarizer (Kogakugiken Corp. WoG-193-E, pol.1) and passed through a MgF_2 sample (l = 20 mm) with/without an external permanent magnet ($\int_0^l Bdl$=1.06 T). MgF_2 crystal is a birefringent material and is optically positively uniaxial. The crystal axis of the sample was cut along the c-axis to prevent unwanted birefringence during measurement. The second polarizer (pol.2), which is of the same type as pol.1, was rotated using a stepper motor. For each measurement step with an angular resolution of 1°, the transmission spectrum ranging at 190–300 nm with a resolution of 0.07 nm was captured using a DUV spectrometer (Ocean Insight Maya200). The direction of rotation of the polarizer is clockwise with respect to the direction of applied the magnetic field. The transmission intensity of the light beam after being polarized by pol.2 without an external magnet can be expressed as:

$$\boldsymbol{I_N(\theta,\lambda) = I_0(\lambda)\cos^2(\theta+\theta_0) + I_{min}(\lambda)}, \tag{2}$$

where I_0 is the maximum intensity, θ is the rotation angle of pol.2, θ_0 is the angular difference between pol.1 and pol.2, and I_{min} is the minimum intensity determined by the extinction ratio of the polarizers. By applying an external magnetic field, polarization rotation θ_F occurs as a result of the Faraday effect, and the above equation changes to

$$\boldsymbol{I_B(\theta,\lambda) = I_0(\lambda)\cos^2(\theta+\theta_0+\theta_F(\lambda)) + I_{min}(\lambda)}. \tag{3}$$

Figure 2 shows a typical data obtained at a wavelength of 248 nm in the spectrum. $\theta_F(\lambda)$ is determined by evaluating the angular difference between the two measurements at each wavelength, and the Verdet constant dispersion can be derived from Eq. (1).

Optics EXPRESS

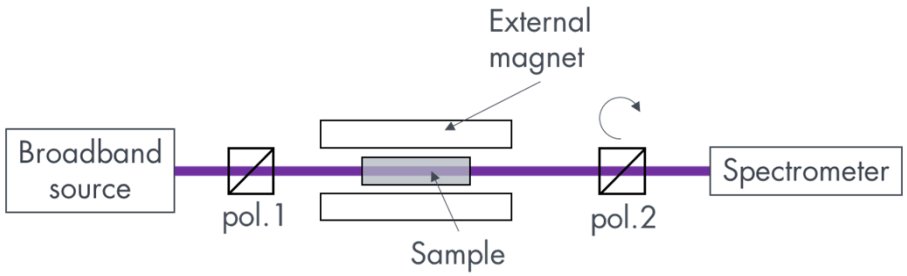

Fig. 1. Experimental setup for the Verdet constant measurement.

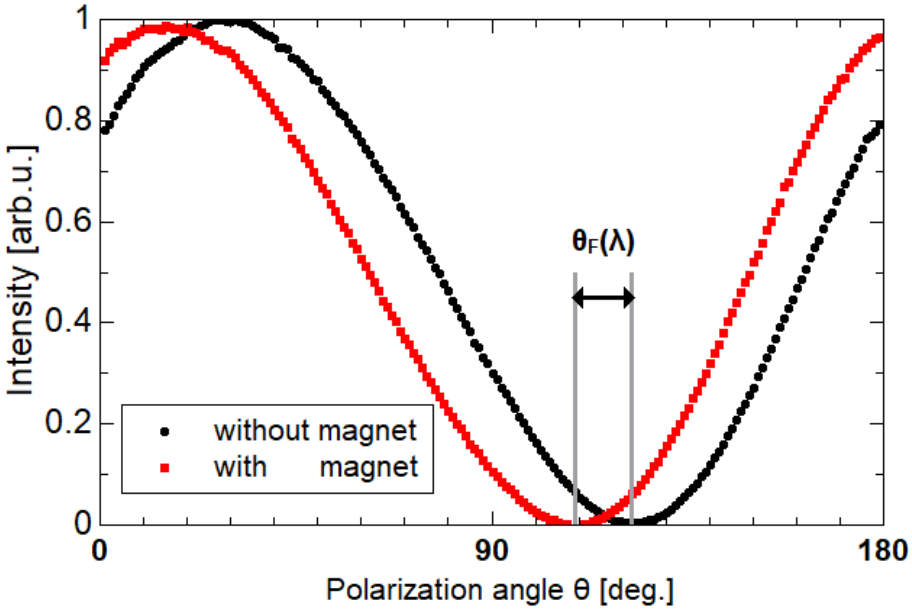

Fig. 2. Typical data of the measurement at a wavelength of 248 nm.

3. Results and discussion

Figure 3 shows the wavelength dependence of the Verdet constant for MgF_2. Table 1 shows the values for typical DUV and VUV light sources, such as excimer lasers and solid-state lasers. The dispersion of the light beam passing through MgF_2, which is a diamagnetic material, can be approximated using the Sellmeier equation for the refractive index [23].

$$V(\lambda) = \frac{\pi}{\lambda} \frac{\{n(\lambda)^2 - 1\}}{2n(\lambda)} \left[A + \frac{B}{\lambda^2 - \lambda_0^2} \right], \tag{4}$$

where n is the refractive index of the sample (n_o = 1.4277 @ λ = 193 nm, 1.4035 @ λ = 248 nm, 1.3991 @ λ = 266 nm) [24], λ_0 is the UV resonance wavelength, and $A = (1.29 \pm 0.03) \times 10^{-6}$ rad/T and $B = (1.72 \pm 0.03) \times 10^{-19}$ (rad·m^2)/T, $\lambda_0 = 66.7 \pm 0.5$ nm are the fitting parameters. The fitting curve is represented by the red dashed line in Fig. 3. The determination coefficient was R^2=0.997. The curve obtained was in good agreement with previously reported values in visible regions, within an average of 7% [21]. Further, the fitting results can be used to predict the Verdet constant in the VUV region, and the resulting values are shown in Table 1.

Optics EXPRESS

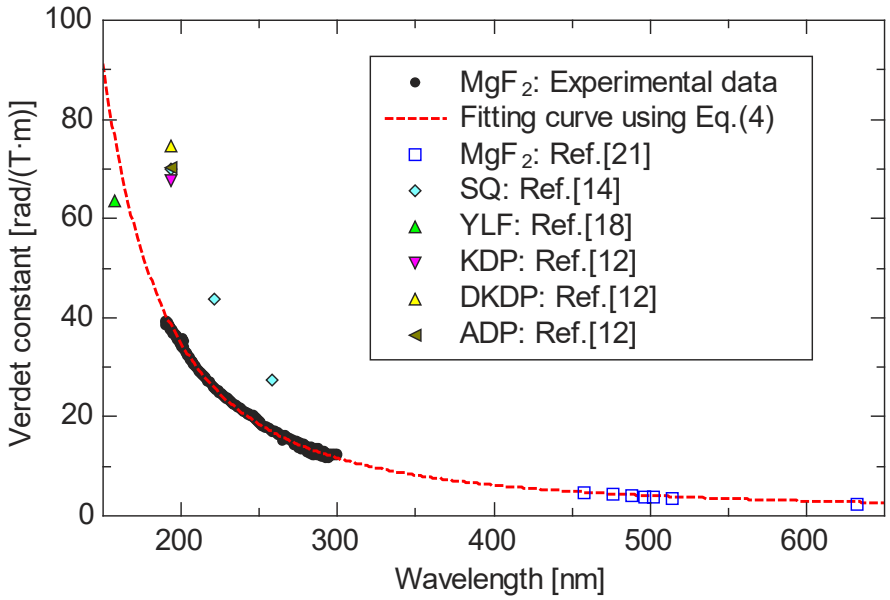

Fig. 3. Dispersion curve of Verdet constants for MgF_2 crystal and other candidate materials.

Table 1. Verdet constant of MgF_2 at the typical DUV and VUV light sources

Laser type	Wavelength [nm]	V [rad/(T·m)]
Third harmonic of Nd:YAG laser	355	7.96 (predict)
XeF	351	8.16 (predict)
XeCl	308	11.0 (predict)
Fourth harmonic of Nd:YAG laser	266	15.7
KrF	248	18.8
Fifth harmonic of Nd:YAG laser	213	28.8
ArF	193	38.7
Xe	172	56.1 (predict)
F_2	157	77.0 (predict)
Fifth harmonic of Ti:sapphire laser by KBBF crystal [6]	149.8	91.1 (predict)
Kr	145	104 (predict)
Ar	125	193 (predict)

Another classical model of dispersion for the Verdet constant was obtained using a modified Becquerel formula derived from classical principles [25].

$$V = \frac{e}{2mc^2}\gamma\lambda\frac{dn}{d\lambda}, \tag{5}$$

where e and m are the electronic charge and mass, respectively, and c is the speed of light. In addition, γ represents the magneto-optic anomaly factor, indicating the nature of the bonding in the crystals. If this value is close to unity, the ionic bond will be predominant. Conversely, when this value is close to 0.28, the covalent bond will be predominant, similar to that of diamond [25]. Based on our measurement results, the γ value was derived as 0.95 ± 0.02 using Eq. (5). This result indicates that the MgF_2 crystals exhibit strong ionic bond, which is comparable to a previous report in the visible region [21].

Optics EXPRESS

The Verdet constant of MgF_2 is relatively small compared to previously reported candidate materials such as SQ glass at the same wavelength ($V_{MgF2} = 38.7$ rad/(T·m), $V_{SQ} = 70.1$ rad/(T·m) at $\lambda = 193$ nm). However, the Verdet constant below a wavelength of 220 nm is above 25 rad/(T·m), which is sufficient to construct FRs with a magnet field strength of 1 T and a medium length of less than 30 mm. Recently, the growth of large MgF_2 crystals, 8 inches diameter with 10 cm thickness, has been reported [26]. In addition, MgF_2 can be used as an FR material in VUV regions because its absorption edge is at a wavelength of 110 nm. For example, the FRs for F_2 lasers ($\lambda = 157$ nm) can be constructed at $l = 10.2$ mm when the magnetic field strength is assumed as $B = 1$ T. However, since the Verdet constants in the VUV region are predicted values, direct measurement in these wavelength regions is necessary to design with high precision. Owing to the large band gap and sufficiently large Verdet constant, MgF_2 is one of the candidate materials in the short-wavelength range of DUV and VUV regions.

4. Conclusions

In summary, we measured the Verdet constant dispersion of MgF_2. This report presents the first measurement of the Verdet constant for MgF_2 in a DUV region. These values are sufficient to construct FRs in DUV regions, especially below a wavelength 220 nm and in VUV regions. Owing to its large band gap and high transmittance, MgF_2 is a promising FR material to be used in DUV–VUV regions. This achievement is expected to break through the lack of magneto-optic devices in DUV-VUV regions. Such devices will be able to contribute to spectroscopy and other areas.

Funding. Amada Foundation (AF-2019221-B3); National Institute for Fusion Science (MISS201).

Disclosures. The authors declare no conflicts of interest.

Data availability. Data underlying the results presented in this paper are not publicly available at this time but may be obtained from the authors upon reasonable request.

References

1. J. Dai and J. Li, "Promising magneto-optical ceramics for high power Faraday isolators," Scr. Mater. **155**, 78–84 (2018).
2. D. Vojna, O. Slezák, A. Lucianetti, and T. Mocek, "Verdet constant of magneto-active materials developed for high-power Faraday devices," Appl. Sci. **9**(15), 3160 (2019).
3. L. Sun, S. Jiang, and J. R. Marciante, "All-fiber optical magnetic field sensor based on Faraday rotation," Opt. Express **18**(6), 5407–5412 (2010).
4. N. C. Pistoni and M. Martinelli, "Vibration-insensitive fiber-optic current sensor," Opt. Lett. **18**(4), 314–316 (1993).
5. E. Munin, "Analysis of a tunable bandpass filter based on Faraday rotators," IEEE Trans. Magn. **32**(2), 316–319 (1996).
6. Y. Kaneda, J. M. Yarborough, L. Li, N. Peyghambarian, L. Fan, C. Hessenius, M. Fallahi, J. Hader, J. V. Moloney, Y. Honda, M. Nishioka, Y. Shimizu, K. Miyazono, H. Shimatani, M. Yoshimura, Y. Mori, Y. Kitaoka, and T. Sasaki, "Continuous-wave all-solid-state 244 nm deep-ultraviolet laser source by fourth-harmonic generation of an optically pumped semiconductor laser using $CsLiB_6O_{10}$ in an external resonator," Opt. Lett. **33**(15), 1705–1707 (2008).
7. H. Turcicova, O. Novak, L. Roskot, M. Smrz, J. Muzik, M. Chyla, A. Endo, and T. Mocek, "New observations on DUV radiation at 257 nm and 206 nm produced by a picosecond diode pumped thin-disk laser," Opt. Express **27**(17), 24286–24299 (2019).
8. Z. Zhang, M. Kushimoto, T. Sakai, N. Sugiyama, L. J. Schowalter, C. Sasaoka, and H. Amano, "A 271.8 nm deep-ultraviolet laser diode for room temperature operation," Appl. Phys. Express **12**(12), 124003 (2019).
9. Y. Uehara, W. Sasaki, S. Saito, E. Fujiwara, Y. Kato, M. Yamanaka, K. Tsuchida, and J. Fujita, "High-power argon excimer laser at 126 nm pumped by an electron beam," Opt. Lett. **9**(12), 539–541 (1984).
10. J. Wieser, D. E. Murnick, A. Ulrich, H. A. Huggins, A. Liddle, and W. L. Brown, "Vacuum ultraviolet rare gas excimer light source," Rev. Sci. Instrum. **68**(3), 1360–1364 (1997).
11. T. Nakazato, I. Ito, Y. Kobayashi, X. Wang, C. Chen, and S. Watanabe, "149.8 nm, the shortest wavelength generated by phase matching in nonlinear crystals," Proc. SPIE **10088**, 1008804 (2017).
12. J. L. Dexter, J. Landry, D. G. Cooper, and J. Reintjes, "Ultraviolet optical isolators utilizing KDP-isomorphs," Opt. Commun. **80**(2), 115–118 (1990).
13. H. Nishioka, H. Hisano, T. Kaminaga, K. Ueda, and H. Takuma, "Development of the UV Faraday Rotator," Rev. Laser Eng. **12**(11), 660–662 (1984).

Optics EXPRESS

14. Y. Tamaru, H. Chen, A. Fuchimukai, H. Uehara, T. Miura, and R. Yasuhara, "Wavelength dependence of the Verdet constant in synthetic quartz glass for deep-ultraviolet light sources," Opt. Mater. Express **11**(3), 814 (2021).
15. P. Molina, V. Vasyliev, E. G. Víllora, and K. Shimamura, "CeF_3 and PrF_3 as UV-Visible Faraday rotators," Opt. Express **19**(12), 11786 (2011).
16. E. G. Víllora, K. Shimamura, and G. R. Plaza, "Ultraviolet-visible optical isolators based on CeF_3 Faraday rotator," J. Appl. Phys. **117**(23), 233101 (2015).
17. V. Vasyliev, E. G. Villora, M. Nakamura, Y. Sugahara, and K. Shimamura, "UV-visible Faraday rotators based on rare-earth fluoride single crystals: $LiREF_4$ (RE = Tb, Dy, Ho, Er and Yb), PrF_3 and CeF_3," Opt. Express **20**(13), 14460 (2012).
18. Y. Tamaru, H. Kumai, A. Fuchimukai, H. Uehara, T. Miura, and R. Yasuhara, "Effect of erbium concentration on the Verdet constant dispersion of $LiY_{1.0-x}Er_xF_4$ single crystal," Opt. Mater. Express **12**(4), 1427 (2022).
19. M. W. Williams, R. A. MacRae, and E. T. Arakawa, "Optical Properties of Magnesium Fluoride in the Vacuum Ultraviolet," J. Appl. Phys. **38**(4), 1701–1705 (1967).
20. A. M. Cook, A. L. Mattioda, R. C. Quinn, A. J. Ricco, P. Ehrenfreund, N. E. Bramall, G. Minelli, E. Quigley, R. Walker, and R. Walker, "Sevo on the ground: Design of a laboratory solar simulation in support of the O/OREOS mission," Astrophys. J. Suppl. Ser. **210**(2), 15 (2014).
21. E. Munin, C. B. Pedroso, and A. B. Villaverde, "Magneto-optical constants of fluoride optical crystals and other AB2 and A2B type compounds," Faraday Trans. **92**(15), 2753 (1996).
22. J. L. Flores and J. A. Ferrari, "Verdet constant dispersion measurement using polarization-stepping techniques," Appl. Opt. **47**(24), 4396–4399 (2008).
23. M. J. Weber, "Faraday rotator materials for laser systems," Proc. SPIE **0681**, 75–90 (1987).
24. H. H. Li, "Refractive index of alkaline earth halides and its wavelength and temperature derivatives," J. Phys. Chem. Ref. Data **9**(1), 161–290 (1980).
25. C. G. Darwin and W. H. Watson, "The constants of the magnetic dispersion of light," Proc. R. Soc. Lond. A **114**(768), 474–490 (1927).
26. M. Cadatal-Raduban, T. Shimizu, N. Sarukura, K. Takahashi, and T. Fukuda, "Crystal growth of ultra-large MgF2 and LiCaAlF6 single crystals by a double-crucible Czochralski technique," J. Cryst. Growth **571**, 126260 (2021).